To appear in: IEEE Transactions on Robotics and Automation, 2003

Nonholonomic Navigation and Control of Cooperating Mobile Manipulators

Herbert G. Tanner Savvas G. Loizou Kostas J. Kyriakopoulos

***Abstract*— This paper presents the first motion planning methodology applicable to articulated, non-point nonholonomic robots with guaranteed collision avoidance and convergence properties. It is based on a new class of nonsmooth Lyapunov functions (DILFs) and a novel extension of the navigation function method to account for non-point articulated robots. The Dipolar Inverse Lyapunov Functions introduced are appropriate for nonholonomic control and offer superior performance characteristics compared to existing tools. The new potential field technique uses diffeomorphic transformations and exploits the resulting point-world topology. The combined approach is applied to the problem of handling deformable material by multiple nonholonomic mobile manipulators in obstacle environment to yield a centralized coordinating control law. Simulation results verify asymptotic convergence of the robots, obstacle avoidance, boundedness of object deformations and singularity avoidance for the manipulators.**

***Index Terms*—Nonholonomic motion planning, cooperative mobile manipulators, potential fields, Inverse Lyapunov Functions.**

I. Introduction

MOTION planning for nonholonomic robots has always been a challenging problem which attracted significant attention over the years [1], [2], [3], [4]. Of particular importance nowadays, given the recent advances in communication and computation capabilities of robotic systems, is the issue of coordinated motion of multiple nonholonomic robotic systems [5], [6], [7]. No general solutions have been proposed for closed loop nonholonomic navigation, especially for multi-robot systems, partly due to the complexity of the problem and the fact that no continuous static control law can stabilize a nonholonomic system to a point [8].

One class of nonholonomic motion planning strategies is based on differential geometry [9], [10], [11], [12], [13]. Flatness properties [14], [15] of nonhonolomic systems have been exploited [16], [17]. Other forms of input parameterization can lead to multi rate [18] and time varying control laws [19], [20], [21], [22], [23], [24], [25]. A significant improvement of the convergence rate of time varying controllers can be achieved by use of homogeneous transformations [26]. On the other hand, the use of discontinuous control laws allows exponential convergence. Such control strategies can be based on appropriately combining different controllers [27], or using nonsmooth transformations of the state space [28], [29].

Herbert Tanner is with the University of Pennsylvania, Department of Electrical and Systems Engineering, Philadelphia PA, USA (e-mail: tanner@grasp.cis.upenn.edu)

Savvas Loizou and Kostas Kyriakopoulos are with the National Technical University of Athens, Greece (e-mail: {sloizou,kkyria}@mail.ntua.gr)

Motion planning strategies developed for obstacle free environments cannot be applied in the presence of obstacles. Typically, the problem is decomposed into *path planning* and *trajectory generation-tracking*. Most of the techniques developed for path planning are classified as geometric path planners [3], [30], [31] with several variations [32], [33], [34], [35]. Solution to the path planning problem is generally sought by graph searching techniques. An alternative methodology is artificial potential fields [36].

Potential fields are reported to yield very good results [3]. Significant effort has been devoted to elimination of local minima [37], [38], [39], [40]. Harmonic potential functions [41] do not exhibit local minima, but they cannot guarantee collision avoidance [42], [43]. Among other techniques [42], particularly interesting is the method of *navigation functions* [44] which is based on a diffeomorphic transformation of the configuration space to a topologically equivalent one, where a globally converging potential function can be constructed. A fundamental difference between geometric path planners and artificial potential fields is that the latter automatically merge path finding and trajectory generation in a closed loop fashion.

Neither of the two classes could directly account for nonholonomic constraints, which could render the planned trajectory infeasible. Sussmann and Liu [45], [46] proved that any collision free path can be approximated by a sequence of feasible nonholonomic paths, that uniformly converges to the original path (although slowly and oscillatory [47]). Another approach [48] replaces the infeasible path with a sequence of Reeds-Shepp [49] paths [50], [51]. If the nonholonomic controllers used satisfy certain topological properties [51], [50] then collision avoidance can still be guaranteed.

Merging path planning and trajectory generation in potential field methods has motivated research towards a nonholonomic potential field controller [52], [53]. De Luca and Oriolo projected the field vector to the direction of admissible motion [54], however, the holonomic nature of potential field flows did not allow the establishment of full state stabilization. To address this problem the authors have introduced the *dipolar potential field* [55]. This approach can be combined with the navigation functions methodology to facilitate the design of globally stabilizing discontinuous nonholonomic controllers [55], [56].

This paper builds on the combination of dipolar potential fields and navigation function methodology to present a new class of nonsmooth potential functions called *Dipolar Inverse Lyapunov Functions*. These functions give rise to nonholonomic controllers with guaranteed obstacle avoidance and convergence properties. Besides being able to handle nonholonomic constraints, such navigation schemes also offer superior

performance compared to existing methodologies. The contributions of this paper are summarized as follows:

1) A new methodology for constructing navigation functions for multi-body, multiple, articulated robots.
2) A new class of navigation functions which are appropriate for nonholonomic motion planning, provide superior performance and require less effort at tuning.
3) Development of a cooperative control scheme for multiple nonholonomic robots operating under various task specifications in an environment with obstacles.

Section II introduces the motivating problem and sets the directions of subsequent analysis. Our first contribution is presented in Section III where we describe a the new methodology for constructing navigation functions for multi-body robotic systems. Section IV defines Dipolar Inverse Lyapunov Functions (DILFs) and establishes their stability-related properties. Section V presents the nonholonomic controller which, based on the methodology of DILFs, solves the motivating problem. Finally, Section VII concludes with a summary of the results.

II. Problem Statement

The results of this paper are motivated by the problem of coordinating the motion of multiple cooperating robotic manipulators in an environment with obstacles under additional task constraints. Towards this end, consider k nonholonomic mobile manipulators, each described kinematically as:

$$\dot{x}_r = v_r \cos\theta_r \tag{1a}$$
$$\dot{y}_r = v_r \sin\theta_r \tag{1b}$$
$$\dot{\theta}_r = \omega_r \tag{1c}$$
$$\dot{\boldsymbol{q}}_{a_r} = \boldsymbol{u}_{a_r}, \quad r = 1, \ldots, k \tag{1d}$$

where (x_r, y_r, θ_r) is the position and orientation of the platform of mobile manipulator r on the plane, v_r and ω_r are the translational and rotational velocities of the mobile platform, $\boldsymbol{q}_{a_r} \in \mathbb{R}^{n_{a_r}}$ the vector of arm joint variables and $\boldsymbol{u}_{a_r}$ the joint rate inputs. Mobile manipulator r configuration is defined as:

$$\boldsymbol{q}_r \triangleq \begin{bmatrix} x_r & y_r & \theta_r & \boldsymbol{q}_{a_r}^T \end{bmatrix}^T \in SE(2) \times S^{n_{a_r}} \triangleq Q_r$$

and the entire system configuration vector is defined as:

$$\boldsymbol{q} \triangleq \begin{bmatrix} \boldsymbol{q}_1 & \ldots & \boldsymbol{q}_k \end{bmatrix} \in \mathcal{Q} \triangleq Q_1 \times \ldots \times Q_k$$

The mobile manipulators are supposed to rigidly grasp a deformable object (Figure 1). Grasp point i is associated with an element $\boldsymbol{s}_i$ of $SE(3)$. An arbitrary grasp frame can serve as the object's floating frame of reference, $\{R\}$ [57]. Without loss of generality we can assume $\boldsymbol{s}_1 \equiv \boldsymbol{s}_R$. With respect to $\boldsymbol{s}_R$, all other grasps can be described by the grasp vector:

$$\boldsymbol{s}(\boldsymbol{q}) \triangleq \begin{bmatrix} \boldsymbol{s}_2(\boldsymbol{q}_2), \ldots, \boldsymbol{s}_k(\boldsymbol{q}_k) \end{bmatrix} \in SE(3) \times \ldots \times SE(3) \tag{2}$$

Each $\boldsymbol{s}_i \in SE(3)$ is a rigid transformation g_i [2].

A finite element decomposition of the deformable object [57] will describe the object shape by means of a set of parameters $\boldsymbol{r}, \boldsymbol{\phi}, \boldsymbol{q}_f$. The first two, $(\boldsymbol{r}, \boldsymbol{\phi})$, correspond to the position and orientation of the object floating frame of reference, while the third, $\boldsymbol{q}_f$, is the vector of (independent) nodal deformations. The object dynamic equations are then obtained in the form:

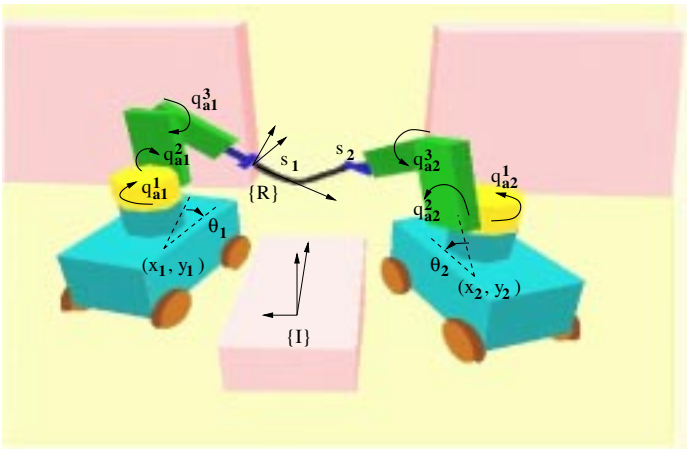

Fig. 1. Mobile manipulators handling a deformable object in an obstacle environment.

$$\begin{bmatrix} \mathsf{m}_r r & \mathsf{m}_{r\phi} & \mathsf{m}_{rf} \\ \mathsf{m}_{r\phi}^T & \mathsf{m}_{\phi\phi} & \mathsf{m}_{\phi f} \\ \mathsf{m}_{rf}^T & \mathsf{m}_{\phi f}^T & \mathsf{m}_{ff} \end{bmatrix} \begin{bmatrix} \ddot{\boldsymbol{r}} \\ \ddot{\boldsymbol{\phi}} \\ \ddot{\boldsymbol{q}}_f \end{bmatrix} + \begin{bmatrix} C_r \\ C_\phi \\ C_f \end{bmatrix} + \begin{bmatrix} 0 & 0 & 0 \\ 0 & 0 & 0 \\ 0 & 0 & \sum_j \mathsf{K}_{ff}^j \end{bmatrix} \begin{bmatrix} \boldsymbol{r} \\ \boldsymbol{\phi} \\ \boldsymbol{q}_f \end{bmatrix} = \begin{bmatrix} Q_r \\ Q_\phi \\ Q_f \end{bmatrix} \tag{3}$$

where m_{ij} are elements of the inertia tensor, C_i are Coriolis and centrifugal vectors, and Q_i are external forces vectors. The dependence of m_{ij}, C_i and Q_i on the object configuration $(\boldsymbol{r}, \boldsymbol{\phi}, \boldsymbol{q}_f)$ and its derivative is dropped for brevity. In (3) the vector of nodal deformations $\boldsymbol{q}_f$ depends on the grasp point coordinates. Since $\boldsymbol{s}_i = (\boldsymbol{p}_i, \mathsf{R}_i) \in SE(3)$, the rigid transformation from the undeformed configuration of grasp i to its deformed can be written as $g_{i1}^0 g_1 g_i^{-1}$, where g_{i1}^0 denotes the (constant) rigid body transformation from the object floating frame of reference to the undeformed grasp. We can express this rigid transformation in terms of the corresponding twist as: $g_{i1}^0 g_1 g_i^{-1} = e^{\hat{\boldsymbol{\xi}}_i \theta_i}$. Extracting the exponential coordinates $\boldsymbol{\xi}_i \theta_i$ we have the contribution of grasp i to the vector of nodal coordinates $\boldsymbol{q}_f$. Without loss of generality, we can assume that we can partition this vector to the grasp-related component $\boldsymbol{q}_f^s = (\boldsymbol{\xi}_2 \theta_2, \ldots, \boldsymbol{\xi}_k \theta_i)$ and the object-related component $\boldsymbol{q}_f^o$. With only gravity forces exerted, the equilibrium configuration $\bar{\boldsymbol{q}}_f$ for the nodal deformations of the object would be:

$$\mathsf{K}_{ff} \bar{\boldsymbol{q}}_f = \boldsymbol{Q}_f \tag{4}$$

and a first order approximation would provide a simplified description of the object kinematics around $\bar{\boldsymbol{q}}_f$:

$$\dot{\boldsymbol{q}}_f^o = -(\mathsf{K}_{ff}^o)^{-1} \mathsf{K}_{ff}^s (\xi_2 \cdots \xi_k)^T$$

with K_{ff}^o guaranteed nonsingular by the reference conditions on the finite element model [57]. Due to material strength limitations the object deformation should remain bounded:

$$\|\boldsymbol{q}_f\|_\infty \leq q_F \tag{5}$$

The problem can now be stated as follows:

Given a group of k planary moving nonholonomic mobile manipulators grasping a deformable object, find a feedback kinematic control law that steers the system in a cooperative manner between two configurations in a known static environment with obstacles such that the object deformation remains within certain bounds.

Towards this goal, we present a novel approach to navigation of nonholonomic systems that builds on a new kind of potential field functions called Dipolar Inverse Lyapunov Functions (DILFs). To handle the volume and the articulated nature of the robots we develop a new methodology for constructing navigation functions and subsequently derive a discontinuous kinematic feedback control law that guarantees global asymptotic stability for the closed loop system.

III. A Potential Field for Non-Point Robots

Creating an artificial potential field requires a mathematical representation of the system and its environment. Existing potential field methods are based on the assumption that the system can be represented by a point in the workspace. For articulated mechanisms and multi robot systems, this is rarely the case. The method presented in this section builds on and extends the navigation function approach of Rimon and Koditschek [44]. It is used to create navigation functions for multi-body articulated robots through a series of diffeomorphic transformations. The sphere-world topology of [44] is pushed to point-world allowing the transformed robots to be treated as points and eliminating the appearance of local minima.

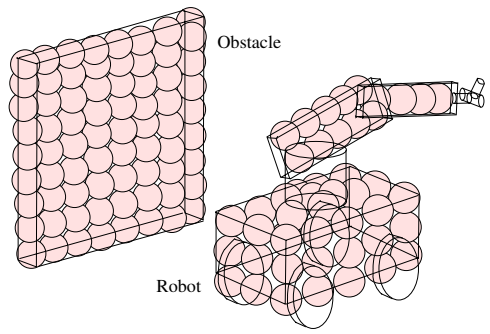

Fig. 2. Robots and obstacles are represented as unions of ellipsoids.

In the approach followed in this paper, the shape of the robotic system $\mathcal{R}$ and the obstacles $\mathcal{O}$ in a three dimensional workspace $\mathcal{W} \subset \mathbb{R}^3$ are considered as unions of generalized n-ellipsoids: $\mathcal{R} = \bigcup_{j\in\mathcal{J}} \mathcal{R}_j$ and $\mathcal{O} = \bigcup_{i\in\mathcal{I}} \mathcal{O}_i$, with $\mathcal{J} = \{1, \ldots, N_R\}$ being the index set of the ellipsoids covering the robots volume and $\mathcal{I} = \{1, \ldots, N_O\}$ the index set of the ellipsoids covering the obstacles' volume (Figure 2). In a reference frame aligned with an ellipsoid's semiaxes, the ellipsoid can be described as a zero level set of a real valued function of the form $b(x, y, z) = 0$:

$$\left(\frac{x-x_0}{a}\right)^{2n} + \left(\frac{y-y_0}{b}\right)^{2n} + \left(\frac{z-z_0}{c}\right)^{2n} - 1 = 0,$$

where a, b, c, x_0, y_0 and z_0 are parameters and $n \geq \frac{1}{2}$. The position and orientation of $\mathcal{R}_j$ is specified by $\boldsymbol{q}$. The boundary of $\mathcal{R}_j$ is described as the zero level set of a real valued function $b_{R_j}(\boldsymbol{q}, x, y, z)$. Accordingly, $\partial\mathcal{O}_i$ is given as $b_{O_i}(x, y, z) = 0$. Functions $b_{R_j}(\boldsymbol{q}, x, y, z)$ and $b_{O_i}(x, y, z)$ are negative in the interior of the respective ellipsoid, vanish on the surface and increase monotonically away from it.

When many independently actuated rigid bodies move in the same workspace, their representation becomes problematic. The solution is given by observing that each moving body has its own "interpretation" of the surrounding world. For each body, any other body, moving or stationary, is an obstacle. Under that perspective, the original workspace is in fact the result of an embedding of all such individual subjective views of the world into a single three dimensional space. Hence, in order to be able to design the motion of each rigid body, we first need to untangle these views and treat them separately.

For each rigid body p of the robotic system we define a special copy of the workspace $\mathcal{W}^p$ (Figure 3(b)). In each $\mathcal{W}^p$ a sequence of smooth transformations yields spaces where the robot part and all obstacles are represented by points. First, the volume of each robot part is reduced to a point (Figure 3(c)). Then, all obstacles "seen" by the robot part are also reduced to points (Figure 3(d)). In the resulting point worlds, navigation functions can be defined and their construction and tuning are easier than in sphere worlds.

A. Transformation to Point-World

For an arbitrary workspace $\mathcal{W}^p$, let $\mathcal{O}_i^p$, $i \in \mathcal{I}^p$ be the ellipsoids that in this particular workspace are treated as obstacles and $\mathcal{R}_j^p$, $j \in \mathcal{J}^p$ the ellipsoids on the rigid body p. If we need to control the orientation of p explicitly, then we can form groups $\mathcal{R}_j^{p_m} \subseteq \mathcal{R}_j^p$ and define separate $\mathcal{W}^{p_m}$ for each group, such that $\mathcal{W}^{p_m} \cap \mathcal{R}_j^p = \mathcal{R}_j^{p_m}$. Then, controlling the position of each $\mathcal{R}_j^{p_m}$ we impose a specific orientation. In a reference frame aligned with the ellipsoid semiaxes, $\mathcal{R}_j^p$ is given by the function:

$$b_{R_j}^p(x, y, z) = \frac{(x-x_j)^{2n}}{a^{2n}} + \frac{(y-y_j)^{2n}}{b^{2n}} + \frac{(z-z_j)^{2n}}{c^{2n}} - 1$$

In this frame, the transformation $\mathcal{H}_0^p(x, y, z)$:

$$\left[\frac{(x-x_j)^n}{a^n} + x_j, \frac{(y-y_j)^n}{b^n} + y_j, \frac{(z-z_j)^n}{c^n} + z_j\right]^T \triangleq \boldsymbol{h}_0^p$$

maps $\mathcal{R}_j^p$ to a unit sphere centered at $\boldsymbol{h}_j = (x_j, y_j, z_j)^T$. This unit sphere is reduced to the point $\boldsymbol{h}_p \in \bigcup_{\mathcal{J}^p} \mathcal{R}_j^p$ through the transformation $\boldsymbol{T}_{R_j}^p(\boldsymbol{h}_0^p)$:

$$\boldsymbol{T}_{R_j}^p(\boldsymbol{h}_0^p) \triangleq \left(\frac{b_{R_j}^p}{b_{R_j}^p + 1}\right)^{\frac{1}{2}} (\boldsymbol{h}_0^p - \boldsymbol{h}_j) + \boldsymbol{h}_p,$$

In an appropriate coordinate system, we can assume that the desired configuration for every $\boldsymbol{h}_p$ is the origin. Define the analytic switches [44]:

$$\sigma_{R_j}^p \triangleq \frac{\|\boldsymbol{h}_p\| \prod_{i\neq j} b_{R_i}^p}{\|\boldsymbol{h}_p\| \prod_{i\neq j} b_{R_i}^p + \lambda b_{R_j}^p}, \tag{6}$$

where λ is a parameter. The transformation $\mathcal{H}_1^p : \boldsymbol{h}_0^p \mapsto \boldsymbol{h}_1^p$:

$$\mathcal{H}_1^p(\boldsymbol{h}_0^p) \triangleq \boldsymbol{h}_1^p = \boldsymbol{h}_0^p(1 - \sum_{j \in \mathcal{J}^p} \sigma_{R_j}^p) + \sum_{j \in \mathcal{J}^p} \sigma_{R_j}^p \boldsymbol{T}_{R_j}^p \quad (7)$$

reduces rigid body p to the point $\boldsymbol{h}_p$ (Figure 3(c)).

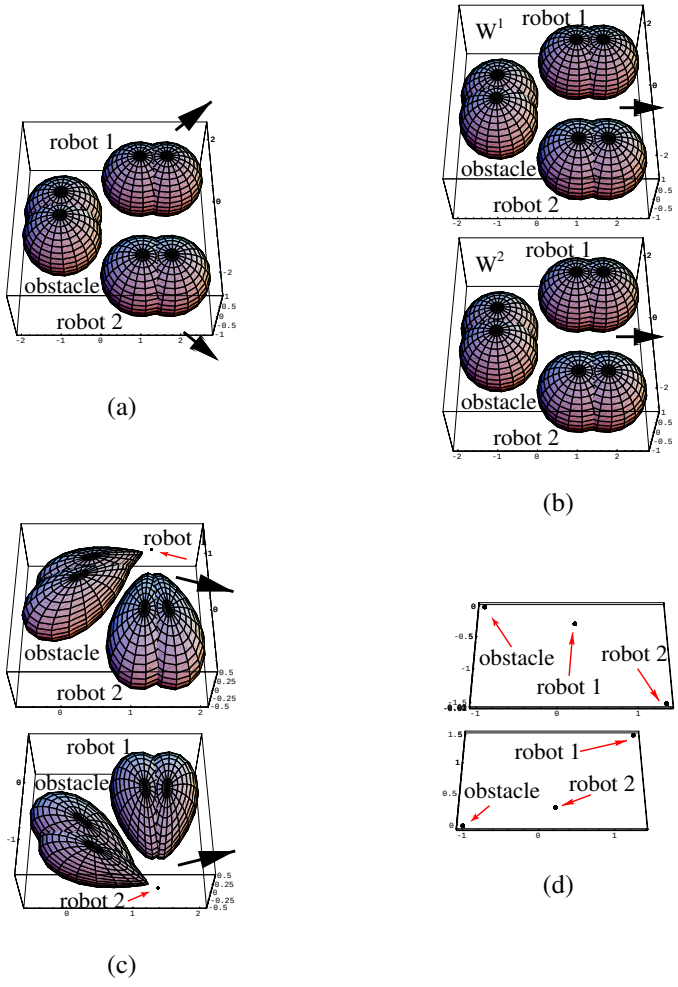

Fig. 3. (a): Original workspace; (b) Workspace copies for each rigid body; (c) Rigid body reduced to point; (d) Deformed obstacles reduced to points.

Remark 1. *Bearing in mind that we will need to differentiate the potential function at $\boldsymbol{h}_p$ we have to ensure that the inverse transformation $(\mathcal{H}_1^p)^{-1}$ exists and is smooth. The inverse mapping of each $\boldsymbol{T}_{R_j}^p$ is given as:*

$$\boldsymbol{h}_0^p = \left(\frac{\|\boldsymbol{T}_{R_j}^p - \boldsymbol{h}_p\|^2 + 1}{\|\boldsymbol{T}_{R_j}^p - \boldsymbol{h}_p\|^2} \right)^{\frac{1}{2}} (\boldsymbol{T}_{R_j}^p - \boldsymbol{h}_p)$$

and regardless of the fact that the inverse image of $\boldsymbol{h}_p$ cannot be directly calculated, there is a limit that depends on the direction of approach to $\boldsymbol{h}_p$. To see that, express $\boldsymbol{T}_{R_j}^p - \boldsymbol{h}_p$ in polar coordinates and verify that: $\lim_{r \to 0} \boldsymbol{h}_0^p = [\cos\theta \cos\phi, \sin\theta \cos\phi, \sin\phi]^T$, where r, θ, ϕ are the polar coordinates. The switches are not defined on the intersection of $\mathcal{R}_j^p$ but the limit exists in this case too. In fact, with some additional computational cost one can isolate each $\mathcal{R}_j^p$ by embedding it to its own workspace and ignoring its immediately neighboring ellipsoids. At any case, the existence of the limits ensures that the transformation $\mathcal{H}_1^p$ is diffeomorphic.

Transformation $\mathcal{H}_1^p$ deforms the shape of $\mathcal{O}_i^p$ in $\mathcal{W}^p$ (Figure 3(c)). The next transformation reduces the deformed $\mathcal{O}_i^p$ to points. Define the analytic switches,

$$\sigma_{O_i}^p \triangleq \frac{\|\boldsymbol{h}_1^p\| \prod_{j \neq i} b_{O_j}^p}{\|\boldsymbol{h}_1^p\| \prod_{j \neq i} b_{O_j}^p + \lambda b_{O_i}^p}, \quad (8)$$

and the mappings,

$$\boldsymbol{T}_{O_i}^p(\boldsymbol{h}_1^p) = \left(\frac{b_{O_i}^p}{b_{O_i}^p + 1} \right)^{\frac{1}{2}} (\boldsymbol{h}_1^p - \boldsymbol{h}_{O_i}) + \boldsymbol{h}_{O_i},$$

where $\boldsymbol{h}_{O_i}$ is common for every set of intersecting $\mathcal{O}_i$. Then the transformation $\mathcal{H}_2^p : \boldsymbol{h}_1^p \mapsto \boldsymbol{h}_2^p$:

$$\mathcal{H}_2^p(\boldsymbol{h}_1^p) \triangleq \boldsymbol{h}_2^p = \boldsymbol{h}_1^p(1 - \sum_{i \in \mathcal{I}^p} \sigma_{O_i}^p) + \sum_{i \in \rangle^p} \sigma_{O_i}^p \boldsymbol{T}_{O_i}^p, \quad (9)$$

reduces $\mathcal{O}_i^p$ into points and translates $\boldsymbol{h}_p$ (Figure 3(d)). Successive application of (7) and (9) yield workspaces $\mathcal{W}_p$ where the robot part and its obstacles are represented by points. A measure of proximity of robot part p to the obstacles could be:

$$d_p(\boldsymbol{h}_2^p) \triangleq \prod_{i \in \mathcal{I}^p} \|\boldsymbol{h}_2^p - \boldsymbol{h}_{O_i}\|$$

A possible choice for a navigation function is [44]:

$$\varphi = \frac{\prod_p \|\boldsymbol{h}_2^p\|^2}{[\prod_p \|\boldsymbol{h}_2^p\|^{2k_v} + \prod_p d_p(\boldsymbol{h}_2^p)]^{\frac{1}{k_v}}} \quad (10)$$

where k_v a tuning constant parameter.

B. Bounded Object Deformation

The object is modeled like the manipulator structure, assigning a group of ellipsoids $\mathcal{R}_j^{f_i}$ to each of the nodes $\boldsymbol{q}_{f_i}$ in the deformable object. The position of each ellipsoid $\mathcal{R}_j^{f_i}$ that represents part of the object's volume is determined by the grasp vector $\boldsymbol{s}$ through (4).

Equation (5) prescribes upper bounds for node deformations. These upper bounds can be rewritten as spatial tolerances for ellipsoids $\mathcal{R}_j^{f_i}$. These tolerances define admissible regions for $\mathcal{R}_j^{f_i}$ which when pushed through $\mathcal{H}_1^{f_i}$ can be underapproximated by balls centered at the undeformed configuration $\bar{\boldsymbol{h}}_{f_i}$ (Figure III-B). This way, condition (5) can be translated into a more conservative constraint of the form:

$$(h_{F_i})^2 - \|\boldsymbol{h}_{f_i} - \bar{\boldsymbol{h}}_{f_i}\|^2 \geq 0 \quad (11)$$

Constraint (11) can be expressed as an obstacle for $\mathcal{R}_j^{f_i}$:

$$b_f \triangleq \prod_i [(h_{F_i})^2 - \|\boldsymbol{h}_{f_i} - \bar{\boldsymbol{h}}_{f_i}\|^2] \quad (12)$$

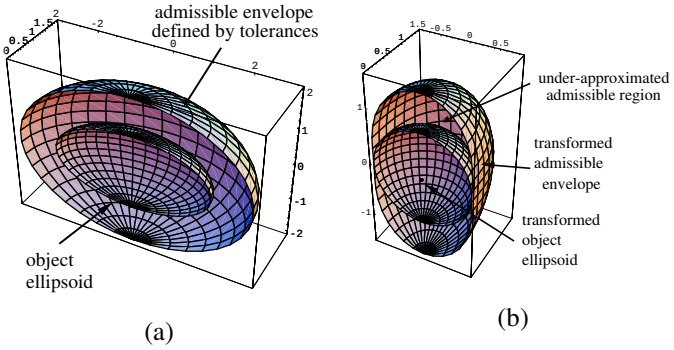

(a) (b)

Fig. 4. (a): An object ellipsoid inside its tolerance envelope; (b) the transformed ellipsoid in its spherical admissible region.

C. Singularity Avoidance

Singularity avoidance can be achieved by representing singularities as artificial obstacles. This has been one of the primary functions of artificial potential fields ever since their first appearance in literature [36]. Singularity regions are sets of measure zero within the configuration space but their shape and location depends on the mechanical structure and cannot be generically described for an arbitrary mechanism. In well designed manipulators, internal singularity regions are generally confined and in many cases they can be decoupled to classes that depend on a subset of the configuration variables [58]. In such cases it is always possible to enclose the singularity regions inside ellipsoids $\mathcal{O}_i^s$ representing artificial obstacles affecting the motion of the robot end-effector.

Singularities can be characterized as solutions of the equation: $\det\left(\mathsf{J}^T\mathsf{J}\right)=0$, where J denotes the Jacobian of the robot. One can consider either the composite Jacobian of the platform-arm system or solely the manipulator Jacobian. Ellipsoids $\mathcal{O}_i^s$ are reduced into points $\boldsymbol{h}_{s_i}$ by $\mathcal{H}_2^p$ and singularity avoidance is ensured by introducing the artificial obstacles:

$$b_s^p \triangleq \prod_i \|\boldsymbol{h}_2^p - \boldsymbol{h}_{s_i}\|^2 \tag{13}$$

for all rigid bodies p in the robotic system.

IV. Dipolar Inverse Lyapunov Functions

Conventional artificial potential fields that have appeared in literature can provide solutions for the problem of navigation of a holonomic point-robot in an obstacle environment [3], [44]. However, none of these methods can take into account the nonholonomic constraints that may be imposed on the robot. As a result, desired motion directions dictated by the potential fields may be infeasible. Application of a feedback controller based on such conventional artificial potential fields could result in the robot being immobilized in configurations that do not constitute local minima for the potential function. In the remaining section we will present a new kind of potential fields that are appropriate for nonholonomic navigation. This kind of potential fields give rise to a new class of nonsmooth Lyapunov functions (ILFs) which can be combined with nonholonomic controllers to yield global asymptotic stability to a destination configuration with collision avoidance.

A. Dipolar Potential Functions

A dipolar potential function is a nonsmooth function, designed so that the potential field at the origin is aligned to the direction of the desired orientation for the vehicle (Figure IV-A). Nonlinear scaling can produce a vector field that allows the development of a globally stabilizing state feedback control law.

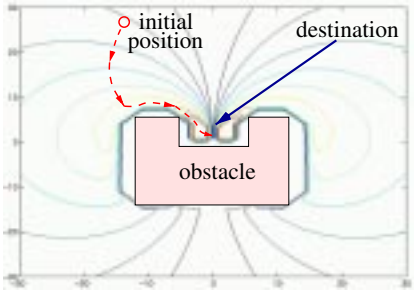

Fig. 5. A dipolar potential field around an obstacle.

Control laws derived from dipolar potential functions do not avoid the need for the vehicle to rotate in place under a certain combinations of initial conditions, including $(x,y,\theta)=(0,0,\phi)$. They can guarantee however that under *all* initial conditions, the vehicle will approach the destination asymptotically and in the process it will follow a path that automatically stabilizes its orientation. Rotation in place will only be necessary at initial time if required by the initial conditions.

Dipolar potential functions can be directly constructed from conventional navigation functions [44] by treating the hyperplane the normal vector of which is parallel to the desired orientation, as an artificial obstacle. For the case of a single robot, this "artificial obstacle" should separate the configuration space to exactly two connected regions. In the multi-robot case the configuration space has to be partitioned into $2k$ connected regions, each containing the origin. Let $\boldsymbol{h}_{c_r}$ denote the point where the platform of mobile manipulator r is transformed into and define the separating surface Γ:

$$\Gamma \triangleq \{\boldsymbol{h}_2^{c_r} \mid \langle (1,0,0)^T, \boldsymbol{h}_2^{c_r}\rangle = 0\},$$

where $\langle\cdot\rangle$ denotes inner product and $\boldsymbol{h}_2^{c_r}$ is the image of $\boldsymbol{h}_{c_r}$ under $\mathcal{H}_2^{c_r}$. Since the analytic switches (6) and (8) vanish at the origin, $\mathcal{H}_1^{c_r}$ and $\mathcal{H}_2^{c_r}$ become the identity there. By continuity, $\frac{\partial\Gamma}{\partial x}\Big|_{\mathbf{0}} = (1,0,0)$ and hence Γ is normal to the direction of desired platform orientation. Defining the artificial obstacle as:

$$\gamma_r \triangleq |\langle (1,0,0)^T, \boldsymbol{h}_2^{c_r}\rangle|, \quad r=1,\ldots,k$$

then in view of (10), (12), (13), a dipolar potential function can be formed as:

$$\varphi_d = \frac{\prod_p \|\boldsymbol{h}_2^p\|^2}{[\prod_p \|\boldsymbol{h}_2^p\|^{2k_v} + b_f \prod_p d_p(\boldsymbol{h}_2^p) b_s^p(\boldsymbol{h}_2^p) \prod_{r=1}^k \gamma_r]^{\frac{1}{k_v}}} \tag{14}$$

B. Inverse Lyapunov Functions

Navigation functions serve as Lyapunov function candidates. The ability to construct navigation functions is important because it provides straightforward stability results. However,

navigation functions require tuning for elimination of local minima. Tuning generally affects convergence rate and can be difficult, especially in multi-dimensional spaces where one can not have visual representation of the navigation function.

Alternative classes of Lyapunov function candidates can be constructed. One such class is *Inverse Lyapunov Functions (ILF)* (Figure 6). An ILF can be derived from a dipolar navigation function, so that it is positive semi-definite, vanishing on the boundary of the admissible space and tending to infinity at the desired configuration:

Definition 1. *Let $\mathcal{D} \subset \mathbb{R}^n$ be a domain containing the origin and consider a real smooth valued function $V(x) : \mathcal{D} \setminus \{\mathbf{0}\} \to \mathbb{R}^+$ having the following properties:*

(i) $V(x) \geq 0, \forall x \in \mathcal{D}$,
(ii) $\lim_{x \to 0} V(x) = +\infty$,
(iii) $\dot{V}(x) > 0, \forall x \in \mathcal{D} \setminus \{0\}$

Function V is called Inverse Lyapunov Function (ILF).

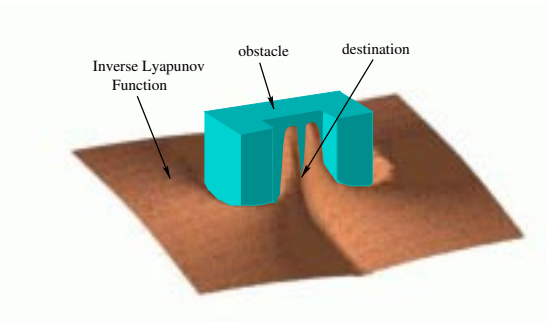

Fig. 6. A dipolar Inverse Lyapunov Function build around an obstacle.

Inverse Lyapunov functions are equivalent to typical Lyapunov functions in the sense that the existence of a representative of the one class implies the existence of a counterpart in the other. Their existence implies asymptotic stability for smooth or nonsmooth systems.

Theorem 1. *A (possibly non smooth) Lyapunov function $V(x)$ exists iff an Inverse Lyapunov Function $W(x)$ exists.*

Proof. See Appendix, Section A. □

Theorem 2. *Consider the continuous system $\dot{x} = f(x)$ with $f(0) = 0$ and $\mathcal{D}$ a neighborhood of the origin. If $V : \mathcal{D} \setminus \{0\} \to \mathbb{R}^+$ is a regular Inverse Lyapunov Function then $x(t)$ approaches the origin asymptotically.*

Proof. See Appendix, Section B. □

Theorem 3. *Consider the system $\dot{x} = f(x)$ where f is Lebesgue measurable and essentially locally bounded. Let $x \equiv 0$ be an equilibrium point and $\mathcal{D}$ a neighborhood of 0 and $V : \mathcal{D} \setminus \{0\} \to \mathbb{R}^+ \cup \{+\infty\}$ a locally Lipschitz and regular function for which it holds:*

(i) $V(x) \geq 0, \forall x \in \mathcal{D}$,
(ii) $\lim_{x \to 0} V(x) = +\infty$

Then if $\dot{V}(x(t)) \geq 0, \forall x \in \mathcal{D} \setminus \{0\}$, $x \equiv 0$ is uniformly stable. If in addition $\dot{V}(x(t)) > 0, \forall x \in \mathcal{D} \setminus \{0\}$, then $x \equiv 0$ is asymptotically stable.

Proof. The proof is similar to that of Theorem 2, with the difference that some relations hold almost everywhere. □

A class of ILFs qualify for navigation functions:

Proposition 1. *Consider the potential function: $V_i(x) = \frac{\beta(x)^{\frac{1}{k}}}{\gamma(x)}$, where $\beta(x)$ is the nonnegative obstacle function vanishing in the boundary of the free space, $\gamma(x)$ is the metric in the free space and k a positive parameter. For k large enough, $V_i(x)$ is a navigation function.*

Proof. See Appendix, Section C. □

Proposition 1 and Theorems 2-3 can be used to establish asymptotic convergence and obstacle avoidance properties of a given feedback controller which is based on an ILF. Before being used, the gradient of an ILF has to be scaled in order to satisfy $\nabla V(x) \to 0$ as $x \to 0$. This is done by multiplication with a $\mathcal{KL}$ function of $\|x\|$: $\boldsymbol{f}(x) = \|\boldsymbol{x}\|^k \nabla V_i$ for a sufficiently large $k > 0$. This factor can be the denominator appearing in $\frac{\partial V}{\partial x}$. The reason why an ILF is preferable to its classical counterpart is outlined in the following claims:

Claim 1. *Inverse Lyapunov Functions can achieve faster convergence rates than their classical counterparts.*

Proof. See Appendix, Section D. □

Claim 2. *There is less derivational complexity in the analytical expression of the potential field generated by Inverse Lyapunov Functions.*

Proof. It can be seen from the proof of Claim 1. □

Claim 3. *Inverse navigation functions are more easily tunable.*

Proof. See Appendix, Section E. □

V. Closed Loop Kinematic Controller

In view of (14) a dipolar ILF can be constructed as:

$$V \triangleq \frac{[b_f \prod_p d_p(\boldsymbol{h}_2^p) b_s^p(\boldsymbol{h}_2^p)]^{\frac{1}{k_v}} \prod_{r=1}^{k} \gamma_r}{\sum_p \|\boldsymbol{h}_2^p\|^2} \tag{15}$$

from which the following potential field can be generated:

$$\boldsymbol{f}_s = \left(\sum_p \|\boldsymbol{h}_2^p\|^2 \right)^2 \nabla V \tag{16}$$

that can be pulled back into the configuration space of the robotic system by differentiating V with respect to $\boldsymbol{q}$:

$$\boldsymbol{f} = \begin{bmatrix} \boldsymbol{f}_1^T & \cdots & \boldsymbol{f}_r^T & \boldsymbol{f}_k^T \end{bmatrix}^T \triangleq \left(\sum_p \|\boldsymbol{h}_2^p\|^2 \right)^2 \frac{\partial V}{\partial \boldsymbol{q}} \tag{17}$$

where $\boldsymbol{f}_r = \begin{bmatrix} f_{x_r} & f_{y_r} & f_{\theta_r} & \boldsymbol{f}_{a_r}^T \end{bmatrix}^T$, $r = 1, \ldots, k$. We will need the following lemma:

Lemma 1 ([27]). *Let $\mathcal{M}^1$, $\mathcal{M}^2$ two open and connected subsets of $\mathbb{R}^n$, such that $\mathcal{M}^1 \cup \mathcal{M}^2 = \mathbb{R}^n \setminus \{\mathbf{0}\}$. Let $\boldsymbol{f}^i : \mathcal{M}^i \to \mathbb{R}^n$, $i = 1, 2$ two vector fields and assume there exists a separating surface Γ with $\mathbf{0} \in \Gamma$ and $\Gamma \setminus \{\mathbf{0}\} \subset \mathcal{M}^1 \cap \mathcal{M}^2$. Let $\mathcal{C}^1$, $\mathcal{C}^2$ two*

connected subsets of $\mathbb{R}^n \setminus \Gamma$ *such that* $\mathcal{C}^i \subset \mathcal{M}^i$ *and assume that* $\boldsymbol{f}^i$ *on* Γ *is pointing towards the interior of* $\mathcal{C}^i$ *for* $i = 1, 2$. *Finally, assume that* $\boldsymbol{f}^1$, $\boldsymbol{f}^2$ *are asymptotically stable on* $\mathcal{M}^1$, $\mathcal{M}^2$. *Then, the vector field* $\boldsymbol{f} : \mathbb{R}^n \to \mathbb{R}^n$ *defined as:*

$$\boldsymbol{f}(\boldsymbol{x}) = \begin{cases} \boldsymbol{f}^1(\boldsymbol{x}) & \text{if } \boldsymbol{x} \in (\Gamma \setminus \{\mathbf{0}\}) \cup \mathcal{C}^1 \\ \boldsymbol{f}^2(\boldsymbol{x}) & \text{if } \boldsymbol{x} \in \mathcal{C}^2 \\ \mathbf{0} & \text{if } \boldsymbol{x} = \mathbf{0} \end{cases}$$

is globally asymptotically stable.

Lemma 1 can be extended for more than two vector fields:

Lemma 2. *Let* $\mathcal{M}^i$, $i = 1, \ldots, k$, k *open and connected subsets of* $\mathbb{R}^n$ *such that* $\cup_i \mathcal{M}^i = \mathbb{R}^n \setminus \{\mathbf{0}\}$. *Let* $\boldsymbol{f}^i : \mathcal{M}^i \to \mathbb{R}^n$, $i = 1, \ldots, k$ *be* k *vector fields and assume there exists a separating surface* Γ *with* $\mathbf{0} \in \Gamma$ *and* $\Gamma \setminus \{\mathbf{0}\}$ *a proper subset of* $\cap_i \mathcal{M}^i$. *Let* $\mathcal{C}^i$, k *connected subsets of* $\mathbb{R}^n \setminus \Gamma$ *such that* $\mathcal{C}^i \subset \mathcal{M}^i$. *In addition, assume that* $\boldsymbol{f}^i$ *on* Γ *is pointing towards the interior of* $\mathcal{C}^i$. *If every* $\boldsymbol{f}^i$ *is asymptotically stable on* $\mathcal{M}^i$, *then the vector field* $\boldsymbol{f} : \mathbb{R}^n \to \mathbb{R}^n$:

$$\boldsymbol{f}(\boldsymbol{x}) = \begin{cases} \boldsymbol{f}^j(\boldsymbol{x}) & \text{if } \boldsymbol{x} \in (\Gamma \setminus \{\mathbf{0}\}) \cup \mathcal{C}^j, \quad j = 1, \ldots, k-1 \\ \boldsymbol{f}^k(\boldsymbol{x}) & \boldsymbol{x} \in \mathcal{C}^k \\ \mathbf{0} & \boldsymbol{x} = \mathbf{0} \end{cases}$$

is globally asymptotically stable.

Proof. See Appendix section F. □

The partition of the state space described in Lemma 2 is induced by function γ_r in (15). If in each region $\mathcal{M}^j$ the vector field is asymptotically stable, then by Lemma 2 the system is globally asymptotically stable:

Proposition 2. *Consider* k *systems of the form* (1) *and assume the existence of a dipolar ILF generated potential field,* (17). *Then the following control law guarantees obstacle avoidance and global asymptotic convergence for the combined system:*

$$v_r = k_v \text{sign}\left(f_{x_r} \cos\theta_r + f_{y_r} \sin\theta_r\right) \|\boldsymbol{f}\| \tag{18a}$$

$$\omega_r = \begin{cases} k_o(\theta_{d_r} - \theta_r), & w_r \geq 0, \\ v_r(f_{x_r} \cos\theta_r + f_{y_r} \sin\theta_r)(f_{\theta_r})^{-1}, & w_r < 0 \end{cases} \tag{18b}$$

$$\boldsymbol{u}_{a_r} = \mathsf{K}_a \boldsymbol{f}_{a_r} \tag{18c}$$

where k_v, k_o *positive constants,* K_a *a positive definite constant matrix, and*

$$\theta_{d_r} \triangleq \text{atan2}(-\text{sign}(x_r) f_{y_r}, -\text{sign}(x_r) f_{x_r})$$
$$w_r \triangleq v_r(f_{x_r} \cos\theta_r + f_{y_r} \sin\theta_r) + k_o f_{\theta_r}(\theta_{d_r} - \theta_r)$$

Proof. See Appendix, Section G. □

The above controller ensures global convergence to the destination by alinging the robot motion with the gradient of the dipolar potential field. This alignment ensures that the robot velocities will only vanish at the destination and rotating in place may only happen at the beginning of the motion.

VI. Simulations

The methodology is applied to a system of two mobile manipulators, each consisted of a nonholonomic mobile platform with three DOF and a fully actuated six DOF manipulator (Figure 1) and a deformable beam rigidly grasped by the robots. The task for the robots is to carry a deformable beam while keeping its deformation bounded and avoiding obstacles. The object is modeled using two 3D rectangular beam finite elements [57], in which the nodal displacements correspond to three infinitesimal translations and three infinitesimal rotations. The upper bound for the deformation vector norm is set to $q_F = 4$, which is quite generous to allow for increased maneuverability for the robots and to demonstrate how object deformation can be exploited in a motion planning task. If q_F, had been set at zero, then the beam would have been treated as rigid and convergence to destination might have been impossible. Such a system possesses a total of 18 DOF. In theory, the methodology can be applied to multi-robot systems with different number of robots and DOF; however, the centralized architecture and the complexity of the the potential function may limit the scalability of this controller synthesis method.

Initial and desired configurations are given in Table I.

Initial Configurations								
x_1	y_1	θ_1	q_1^1	q_1^2	q_1^3	q_1^4	q_1^5	q_1^6
-11	3	$-\frac{\pi}{2}$	$\frac{\pi}{2}$	$-\frac{\pi}{2}$	$\frac{2\pi}{3}$	0	$-\frac{\pi}{6}$	0
x_2	y_2	θ_2	q_2^1	q_2^2	q_2^3	q_2^4	q_2^5	q_2^6
-8	3	$-\frac{\pi}{2}$	$-\frac{\pi}{3}$	$-\frac{\pi}{2}$	$\frac{2\pi}{3}$	0	$-\frac{\pi}{4}$	0
Desired Configurations								
x_1	y_1	θ_1	q_1^1	q_1^2	q_1^3	q_1^4	q_1^5	q_1^6
0	-2	0	$\frac{\pi}{3}$	$-\frac{\pi}{2}$	$\frac{2\pi}{3}$	0	$-\frac{\pi}{6}$	0
x_2	y_2	θ_2	q_2^1	q_2^2	q_2^3	q_2^4	q_2^5	q_2^6
0	2	0	$-\frac{\pi}{2}$	$-\frac{\pi}{2}$	$\frac{2\pi}{3}$	0	$-\frac{\pi}{6}$	0

TABLE I
INITIAL AND DESIRED CONFIGURATIONS.

The position error trajectories are given in Figures 18-19. The asymptotic nature of convergence is particularly evident in the evolution of arm joint angles, since the manipulators have to maneuver to avoid obstacles while maintaining contact with the object. Beam deformations are shown in Figure 17. Large rotational deformations are exhibited during the motion in an effort to exploit elasticity for faster convergence. However, in all cases, deformations remain within the specified limits. The robots' motion is captured in successive snapshots given in Figures 7-16. The workspace is structured as an indoor environment and the task for the robots is to transfer the object through a door opening and hold it over a rectangular shaped obstacle. The robots are initially positioned next to each other (Figure 7) and start moving towards the door opening (Figures 8-9) where the robots negotiate their motion through the door via the centralized controller (Figures 10-13). Once inside they maneuver towards the destination configuration (Figures 14-16).

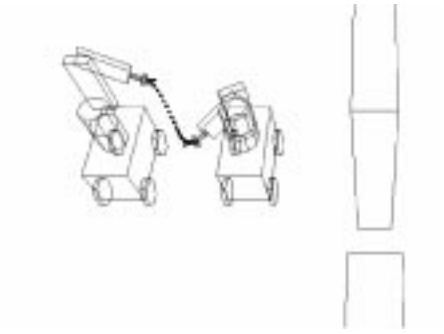

Fig. 7. Time = 0.0 sec.

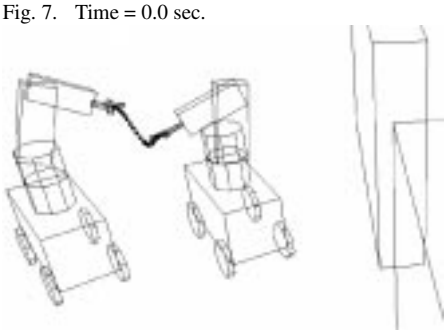

Fig. 8. Time = 0.1 sec.

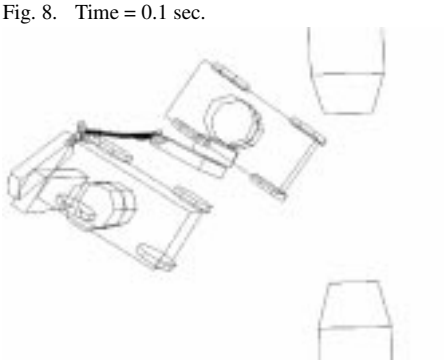

Fig. 9. Time = 4.0 sec.

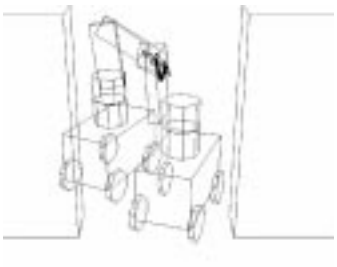

Fig. 10. Time = 6.0 sec.

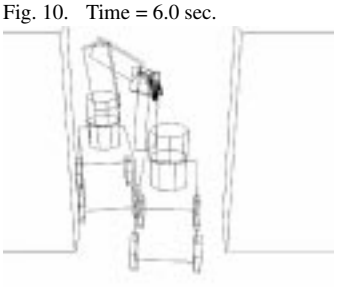

Fig. 11. Time = 7.0 sec.

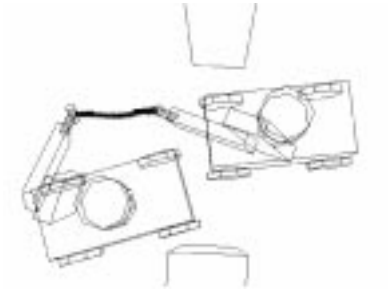

Fig. 12. Time = 8.0 sec.

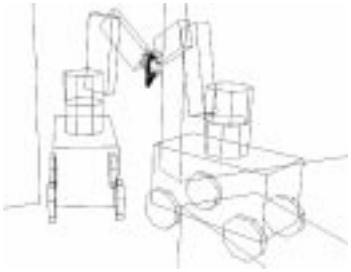

Fig. 13. Time = 12.0 sec.

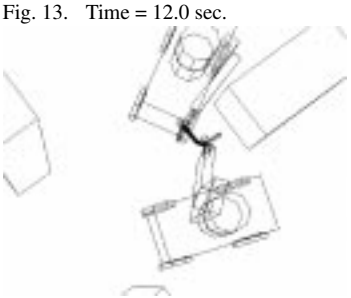

Fig. 14. Time = 16.0 sec.

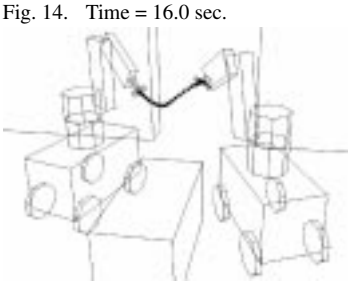

Fig. 15. Time = 24.0 sec.

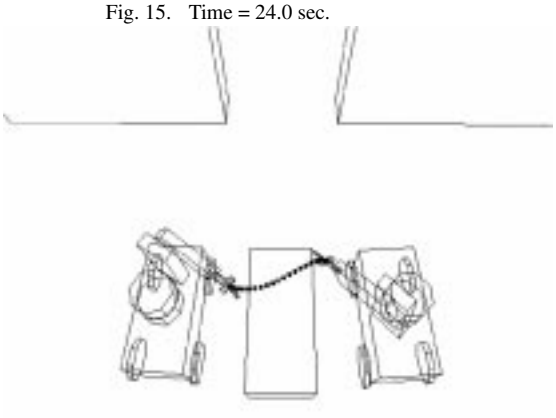

Fig. 16. Time = 50.0 sec.

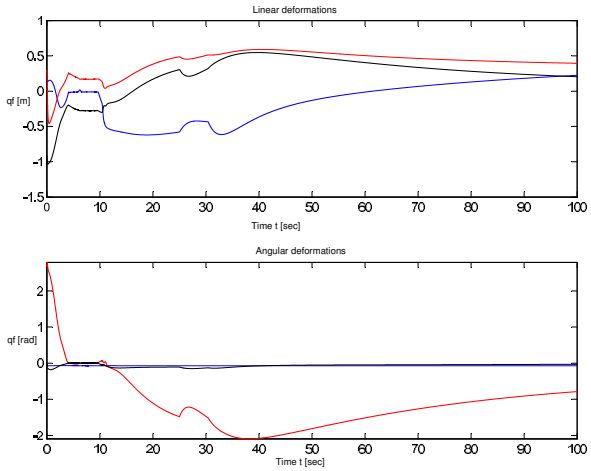

Fig. 17. Deformations at the center of mass of the beam.

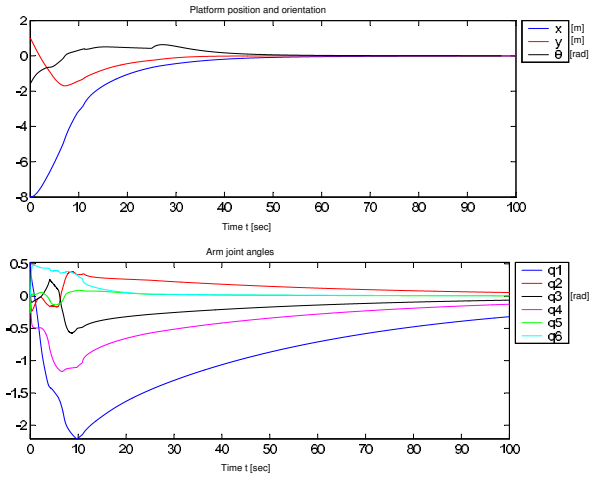

Fig. 19. Platform position (up) and joint angles (down) of robot 2.

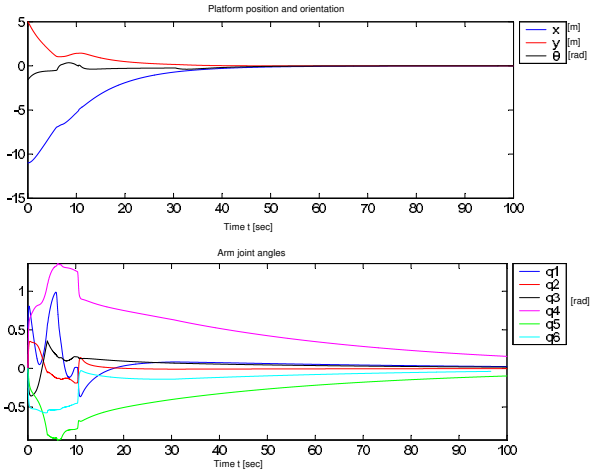

Fig. 18. Platform position (up) and joint angles (down) of robot 1.

VII. Conclusions

This paper presents the first, to the authors' knowledge, methodology for nonholonomic motion planning of articulated, non-point robots in obstacle environments with guaranteed collision avoidance and convergence properties. The methodology is applied to the case of handling of deformable material by multiple nonholonomic mobile manipulators and yields asymptotic convergence of the robots, obstacle avoidance and nonholonomic navigation in cluttered environments, motion coordination for the multi-robot system, boundedness of object deformations and singularity avoidance for the manipulator mechanisms. These objectives are met simultaneously using a new class of nonsmooth artificial potential functions, namely dipolar *Inverse Lyapunov Functions (ILF)*. This new class of potential functions is appropriate for nonholonomic mobile robot motion planning, and allows easier tuning, offers computational savings and yields faster convergence rates. The mathematical representation of the workspace allows modeling the system's volume and its non stationary shape, allowing the treatment of a large class of robots and obstacles. The system is kinematically controlled by a globally asymptotically stable centralized discontinuous state feedback controller, based on the artificial potential field. Stability is analyzed in the framework of nonsmooth Lyapunov theory which, for this purpose, is enriched by useful extensions of recently developed tools. Overall performance is verified through numerical simulations.

Acknowledgments

The work of the first author was partially supported by the Institute of Communication and Computer Systems at NTUA. The authors wish to thank the reviewers and the Editor for their constructive comments.

References

[1] Z. Li and J.F. Canny, *Nonholonomic Motion Planning*, Kluwer Academic Publishers, 1993.

[2] R.M. Murray, Z. Li, and S.S. Sastry, *A Mathematical Introduction to Robotic Manipulation*, CRC Press, 1994.

[3] J.C. Latombe, *Robot Motion Planning*, Kluger Academic Pub., 1991.

[4] I. Kolmanovsky and N.H. McClamroch, "Developments in nonholonomic control problems," *IEEE Control Systems*, pp. 20–36, December 1995.

[5] Jaydev P. Desai, James P. Ostrowski, and Vijay Kumar, "Modeling and control of formations of nonholonomic mobile robots," *IEEE Transactions on Robotics and Automation*, vol. 17, no. 6, pp. 905–908, 2001.

[6] Paulo Tabuada, George J. Pappas, and Pedro Lima, "Feasible formations of multi-agent systems," in *Proceedings of the American Control Conference*, Arlington, VA, June 2001, pp. 56–61.

[7] T. Sugar, J. Desai, V. Kumar, and J. P. Ostrowski, "Coordination of multiple mobile manipulators," in *Proceedings of IEEE International Conference on Robotics Automation*, May 2001, vol. 3, pp. 3022–2027.

[8] R. Brockett, *Control Theory and Singular Riemannian Geometry*, New Directions in Applied Mathematics. Springer, 1981.

[9] G. Lafferriere and H. Sussmann, "Motion planning for controllable systems without drift," in *Proceedings of the 1991 IEEE International Conference on Robotics and Automation*, Apr. 1991.

[10] G.A. Lafferriere and H. Sussmann, "A differential geometric approach to motion planning," in *Nonholonomic Motion Planning*, Z. Li and J.F. Canny, Eds., pp. 235–270. Kluwer Academic Publishers, 1993.

[11] M. Reyhanoglu, "A general nonholonomic motion planning strategy for chaplygin systems," in *33rd IEEE Conference on Decision and Control*, December 1994, pp. 2964–2966.

[12] R.M. Murray, "Applications and extentions of goursat normal form to control of nonlinear systems," in *Proc. of the 32rd IEEE Conference on Decision and Control*, December 1993, pp. 3425–3430.

[13] D. Tilbury, R. Murray, and S. Sastry, "Trajectory generation for the n-trailer problem using goursat normal forms," in *Proc. of the 32rd IEEE Conference on Decision and Control*, December 1993, pp. 971–977.

[14] M. Fliess, J. Lévine, Ph. Martin, and P. Rouchon, "Flatness and defect on nonlinear systems: introductory theory and examples," *International Journal of Control*, vol. 61, no. 6, pp. 1327–1361, 1995.

[15] M. Fliess, J. Lévine, Ph. Martin, and P. Rouchon, "On differentially flat nonlinear systems," in *Proc. of the 3rd IFAC Symposium on Nonlinear Control Systems Design*, Bordeaux, France, 1992, pp. 408–412.

[16] P. Rouchon, M. Fliess, J. Levine, and Ph. Martin, "Flatness, motion planning and trailer systems," in *Proc. of the 32rd IEEE Conference on Decision and Control*, Austin, TX, December 1993, pp. 2700–2705.

[17] P. Rouchon, M. Fliess, J. Levine, and Ph. Martin, "Flatness and motion planning: the car with n trailers," in *Proc. of the European Control Conference*, Groningen, Netherlands, 1992, pp. 1518–1522.

[18] D. Tilbury and A. Chelouah, "Steering a three input nonholonomic system using multirate controls," in *Proc. of the European Control Conference*, Groningen, Netherlands, 1992, pp. 1993–1998.

[19] R.M. Murray and S.S. Sastry, "Nonholonomic motion planning : Steering using sinusoids," *IEEE Transactions on Automatic Control*, pp. 700–716, May 1993.

[20] L. Bushnell, D. Tilbury, and S. Sastry, "Steering three-input chained form nonhonolomic systems using sinusoids," in *Proc. of the European Control Conference*, 1993, pp. 1432–1437.

[21] R. Murray D. Tilbury and S. Sastry, "Trajectory generation for the n-trailer problem using goursat normal forms," *IEEE Transactions on Robotics and Automation*, vol. 40, pp. 802–819, 1995.

[22] J.-M. Coron, "Global asymptotic stabilization for controllable systems without drift," *Mathematics of Control, Signals and Systems*, vol. 5, pp. 295–312, 1991.

[23] J.-P. Pomet, "Explicit design of time-varying stabilizing control laws for a class of controllable systems without drift," *Systems & Control Letters*, vol. 18, pp. 147–158, 1992.

[24] C. Samson, "Velocity and torque feedback stabilization of a nonholonomic cart," in *Advanced Robot Control*, C. Canudas de Wit, Ed., pp. 125–151. Springer, 1991.

[25] P. Morin and C. Samson, "Control of nonlinear chained systems: From the routh-hurwitz stability criterion to time-varying exponential stabilizers," *IEEE Transactions on Automatic Control*, vol. 45, no. 1, pp. 141–146, 2000.

[26] R.T. M' Closkey and R.M. Murray, "Exponential stabilization of driftless nonlinear control systems using homogeneous feedback," *IEEE Transactions on Robotics and Automation*, vol. 42, no. 5, pp. 614–628, 1997.

[27] G.A. Lafferriere and E.D. Sontag, "Remarks on control lyapunov functions for discontinuous stabilizing feedback," in *Proceedings of the 32nd IEEE Int. Conf. on Decision and Control*, San Antonio, TX, 1993, pp. 2398–2403.

[28] C. Canudas de Wit and O.J. Sordalen, "Exponential stabilization of mobile robots with nonholonomic constraints," *IEEE Transactions on Automatic Control*, vol. 13, no. 11, pp. 1791–1797, 1992.

[29] A. Astolfi, "Discontinuous control of nonholonomic systems," *Systems & Control Letters*, vol. 27, pp. 37–45, 1996.

[30] T. Lozano-Pérez and M.A. Wesley, "An algorithm for planning collision free paths among polyhedral obstacles," *Comm. ACM*, vol. 22, no. 10, pp. 560–570, 1979.

[31] K. Kedem and M. Sharir, "An efficient motion planning algorithm for a convex polygonal object in 2-d polygonal space," Technical Report 253, Courant Insitute of Mathematical Sciences, 1986.

[32] L.E. Kavraki, P. Švestka, J.-C. Latombe, and M.H. Overmars, "Probabilistic roadmaps for path planning in high-dimensional configuration spaces," *IEEE Transactions on Robotics and Automation*, vol. 12, no. 4, pp. 566–580, 1996.

[33] J.F. Canny and M.C. Lin, "An opportunistic global path planner," in *Proc. of IEEE Conference on Robotics and Automation*, Cincinnati, OH, 1990, pp. 1554–1559.

[34] D. Zhu and J.-C. Latombe, "New heuristic algorithms for efficient hierarchical path planning," *IEEE Transactions on Robotics and Automation*, vol. 7, no. 1, pp. 9–20, 1991.

[35] J.M. Ahuactzin, E.-G. Talbi, P. Bessière, and E. Mazer, "Using genetic algorithms for robot motion planning," in *Proc. of 10th European Conference on Artificial Intelligence*, London, 1992, pp. 671–675.

[36] O. Khatib, *Commande dynamique dans l'espace opérationnel des robots manipulateurs en présence d'obstacles*, Ph.D. thesis, École nationale Supérieure de l'Aéronatique et de l'Espace (ENSAE), Toulouse, France, 1980.

[37] B.H. Krogh, "A generalized potential field approach to obstacle avoidance control," in *Proc. of SME Conference on Robotics Research*, Bethlehem, PA, 1984.

[38] C.I. Connolly, J.B. Burns, and R. Weis, "Path planning using laplace's equation," in *Proc. of IEEE Conference on Robotics and Automation*, Cincinnati, OH, 1990, pp. 2102–2106.

[39] J. Barraquand and J.-C. Latombe, "A monte-carlo algorithm for path-planning with many degrees of freedom," in *Proc. of IEEE Conference on Robotics and Automation*, Cincinnati, OH, 1990, pp. 1712–1717.

[40] J. Barraquand, B. Langlois, and J.-C. Latombe, "Numerical potential fields techniques for robot path planning," *IEEE Transactions on Systems, Man and Cybernetics*, vol. 22, pp. 224–241, 1992.

[41] J.O. Kim and P.K. Khosla, "Real-time obstacle avoidance using harmonic potential functions," *IEEE Transactions on Robotics and Automation*, vol. 8, no. 3, pp. 338–349, 1992.

[42] L. Singh, H. Stephanou, and J. Wen, "Real-time robot motion control with circulatory fields," in *Proc. of IEEE Conference on Robotics and Automation*, Minneapolis, MN, 1996, pp. 2737–2742.

[43] J.-H. Chuang, "Potential-based modeling of three-dimensional workspace for obstacle avoidance," *IEEE Transactions on Robotics and Automation*, vol. 14, no. 5, pp. 778–785, 1998.

[44] E. Rimon and D. Koditschek, "Exact robot navigation using artificial potential functions," *IEEE Transactions on Robotics and Automation*, vol. 8, no. 5, pp. 501–518, October 1992.

[45] H. Sussmann and W. Liu, "Limits of highly oscilatory controls and the approximation of general paths by admissible trajectories," Report SYCON 91-02, Department of Mathematics, Rutgers University, February 1991.

[46] H. Sussmann and W. Liu, "The bracket extentions and averaging: the single-bracket case," in *Nonholonomic Motion Planning*, Z. Li and J.F. Canny, Eds., pp. 109–147. Kluwer Academic Publishers, 1993.

[47] D. Tilbury, J.P. Laumond, R. Murray, S. Sastry, and G. Walsh, "Steering car-like systems with trailers using sinusoids," in *Proceedings of the 1992 IEEE Conference on Robotics and Automation*, Nice, France, May 1992, pp. 1993–1998.

[48] J.P. Laumond, P.E. Jacobs, M. Taix, and R.M. Murray, "A motion planner for nonholonomic mobile robots," *IEEE Transactions on Robotics & Automation*, vol. 10, no. 5, pp. 577–593, Oct. 1994.

[49] J.A. Reeds and L.A. Shepp, "Optimal paths for a car that goes both forward and backward," *Pacific Journal of Mathematics*, vol. 2, pp. 367–393, 1990.

[50] S. Sekhavat and J.-P. Laumond, "Topological property for collision-free nonholonomic motion planning: The case of sinusoidal inputs for chained form systems," *IEEE Transactions on Robotics and Automation*, vol. 14, no. 5, pp. 671–680, 1998.

[51] J.-P. Laumond, "Singularities and topological aspects in nonholonomic motion planning," in *Nonholonomic Motion Planning*, Z. Li and J.F. Canny, Eds., pp. 149–199. Kluwer Academic Publishers, 1993.

[52] A. De Luca and G. Oriolo, "Local incremental planning for nonholonomic mobile robots," in *Proc. of IEEE Conference on Robotics and Automation*, San Diego, CA, May 1994, pp. 104–110.

[53] K.J. Kyriakopoulos, H.G. Tanner, and N.J. Krikelis, "Navigation of nonholonomic vehicles in complex environments with potential fields and tracking," *International Journal of Intelligent Control and Systems*, vol. 1, no. 4, pp. 487–495, 1996.

[54] A. Bemporad, A. De Luca, and G. Oriolo, "Local incremental planning for car-like robot navigating among obstacles," in *Proc. of IEEE Conference on Robotics and Automation*, Minneapolis, MN, April 1996, pp. 1205–1211.

[55] H.G. Tanner and K.J. Kyriakopoulos, "Nonholonomic motion planning for mobile manipulators," in *Proc. of the 2000 IEEE International Conference on Robotics and Automation*, San Francisco, April 2000, pp. 1233–1238.

[56] H.G. Tanner, S. Loizou, K.J. Kyriakopoulos, K. Arvanitis, and N. Sigrimis, "Coordinating the motion of a manipulator and a mobile base in tree environments," in *Proc. of the IFAC Workshop on Bio-robotics, Information Technology and Intelligent Control for Bioproduction Systems*, Osaka, Japan, November 2000.

[57] A.A. Shabana, *Dynamics of Multibody Systems*, Cambridge, 1998.

[58] L. Sciavicco and B. Siciliano, *Modeling and Control of Robot Manipulators*, McGraw-Hill, 1996.

[59] H. K. Khalil, *Nonlinear Systems*, Prentice Hall, 1996.

APPENDIX

A. Proof of Theorem 1

Let $V(x)$ be a Lyapunov function for the system $\dot{x} = f(x)$, that is:

(i) $V(x) > 0, \quad \forall x \in \mathcal{D} \subset \mathbb{R}^n$,

(ii) $V(x) = 0, \quad$ for $x = 0$,

(iii) $\dot{V}(x) < 0, \quad \forall x \in \mathcal{D} \setminus \{0\}$.

Then we can define the function: $W(x) \triangleq \frac{1}{V(x)}$. It is clear that W satisfies the first two requirements of Definition 1. For the third a direct calculation yields:

$$\dot{W}(x) = \frac{-1}{V^2(x)} \cdot \dot{V}(x) > 0, \quad \forall x \in \mathcal{D} \setminus \{0\}$$

Therefore, $W(x)$ is an Inverse Lyapunov Function.

Conversely, if $W(x)$ is an Inverse Lyapunov Function satisfying the requirements (i)–(iii) of Definition 1, then we can define the function:

$$V(x) \triangleq \begin{cases} \frac{1}{W(x)}, & x \neq 0, \\ 0, & x = 0 \end{cases}$$

By definition, $V(x)$ is continuous at the origin but it may not be smooth. We can say that $V(x)$ is smooth almost everywhere since the origin is a set of measure zero. It is still a valid Lyapunov function since stability requires only continuity at the origin.

B. Proof of Theorem 2

The proof borrows from its classical counterpart in [59]: Let $\varepsilon > 0$. Then there is an $r \in (0, \varepsilon]$ such that $B_r \triangleq \{x \in \mathbb{R}^n \mid \|x\| \leq r\} \subset \mathcal{D}$ Let $\alpha \triangleq \max_{\|x\|=r} V(x)$, choose a $\beta \in (\alpha, +\infty)$ and define: $\Omega_\beta \triangleq \{x \in B_r \mid V(x) \geq \beta\}$ Such a set always exists since $\lim_{x \to 0} V(x) = +\infty$, that implies that for every β there will be a δ for which $\|x\| < \delta \Rightarrow V(x) > \beta$. The set Ω_β lies inside B_r. This can easily be shown by contradiction. Additionally, every trajectory starting in Ω_β remains in Ω_β for all t: $\dot{V}(x) \geq 0 \Rightarrow V(x(t)) \geq V(x(0)) \geq \beta, \forall t \geq 0$ and therefore $x(t) \in \Omega_\beta, \forall t > 0$, if $x(0) \in \Omega_\beta$. Since $V(x) \to +\infty$, if $x \to 0$ then for all $\beta > 0$, there will exist a $\delta > 0$ such that $\|x\| < \delta \Rightarrow V(x) > \beta$. Therefore, $B_\delta \subset \Omega_\beta \subset B_r$ and $x(0) \in B_\delta \Rightarrow x(0) \in \Omega_\beta \Rightarrow x(t) \in \Omega_\beta \Rightarrow x(t) \in B_r$, which establishes the stability of $x = 0$.

To show that $x = 0$ is asymptotically stable, consider a sequence $x(t_n)$, with $t_n \to \infty$. Since $\dot{V}(x) > 0, \forall x \in \mathcal{D} \setminus \{0\}$, then $V(x(t))$ is strictly increasing. $V(x)$ not being bounded from above, so $V(x(t_n)) \to +\infty, t_n \to \infty$, which holds for every sequence $x(t_n)$. Therefore, $V(x(t)) \to \infty$ as $t_n \to \infty$. This means that for every $\beta > 0$, there will be a $T > 0$ such that $V(x(t)) > \beta, \forall t > T$. Since $V(x(t)) > \beta$, there will be $x(t) \in \Omega_\beta \subset B_r$. Thus, $\|x\| \leq r < \varepsilon$. This holds for every $\varepsilon > 0$.

Summarizing: for every $\varepsilon > 0$, there is a $T > 0$ for which $\forall t > T, \|x(t)\| < \varepsilon$. As a result, the origin is asymptotically stable.

C. Proof of Proposition 1

The gradient of V_i is :

$$\nabla \left(\frac{\beta^{\frac{1}{k}}}{\gamma} \right) = \frac{k^{-1} \beta^{\frac{1}{k}-1} \nabla\beta \cdot \gamma - \beta^{\frac{1}{k}} \nabla\gamma}{\gamma^2}$$

At a critical point it would be:

$$\nabla V_i = 0 \Rightarrow k^{-1} \beta^{\frac{1}{k}-1} \nabla\beta \cdot \gamma - \beta^{\frac{1}{k}} \nabla\gamma = 0 \qquad (19)$$

Examining the Hessian:

$$\nabla^2 V_i = \frac{\left(\frac{\gamma}{\beta^2} (\nabla\beta)^2 + k \frac{\gamma}{\beta} (\nabla^2\beta - \frac{1}{\beta} (\nabla\beta)^2) - k^2 \nabla^2\gamma \right) \beta^{\frac{1}{k}}}{\gamma^2 k^2}$$

The nature of the critical points is thus determined by the matrix $F = \gamma\beta^{-2}(\nabla\beta)^2 + k\gamma\beta^{-1}(\nabla^2\beta - \beta^{-1}(\nabla\beta)^2) - k^2\nabla^2\gamma$. If $F > 0$, then the critical points are local minima and since the system is attracted to the maximum of the ILF, the points would be repulsive. In fact, $F > 0$, is a special case of the linear matrix inequality (LMI):

$$\gamma\beta^{-2}(\nabla\beta)^2 + x_1\gamma\beta^{-1}(\nabla^2\beta - \beta^{-1}(\nabla\beta)^2) - x_2\nabla^2\gamma > 0$$

For any positive semidefinite $G \neq 0$, $\mathrm{Tr}(\frac{\gamma}{\beta^2} G(\nabla\beta)^2) \geq 0$ and $\mathrm{Tr}(G\nabla^2\gamma) \neq 0$, and so the LMI has a nonempty solution set. Note that $k \to 0$ implies $F > 0$ and therefore 0 belongs in the solution set. Thus, a sufficiently small k can ensure that all critical points are repulsive.

D. Proof of Claim 1

For clarity of presentation, consider the case of no obstacles: $\beta \equiv 1$. A classical navigation function can be expressed as:

$$\varphi = \frac{\|x\|^2}{(\|x\|^{2k} + 1)^{\frac{1}{k}}}$$

The potential field produced is:

$$\nabla\varphi = \frac{2\|x\|[\nabla\|x\|(\|x\|^{2k} + 1)^{\frac{1}{k}} - \|x\|^{2k+1}(\|x\|^{2k} + 1)^{\frac{1-k}{k}}]}{(\|x\|^{2k} + 1)^{\frac{2}{k}}}$$

whereas for an Inverse Lyapunov Function, $\varphi_i = \frac{1}{\|x\|^2}$:

$$f(x) = \|x\|^4 \nabla\varphi_i = -2\|x\|\nabla\|x\|$$

recovering an exponential rate of convergence for $\|x\|$. Thus, under the same environment conditions, $\|x\|$ is decreasing faster along the flows of the ILF potential field.

E. Proof of Claim 3

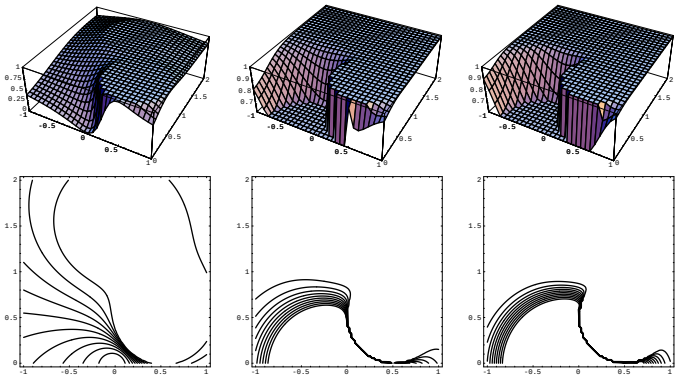

Fig. 20. Shape of a classical navigation function for parameter k taking values $1, 5, 10$ (left to right).

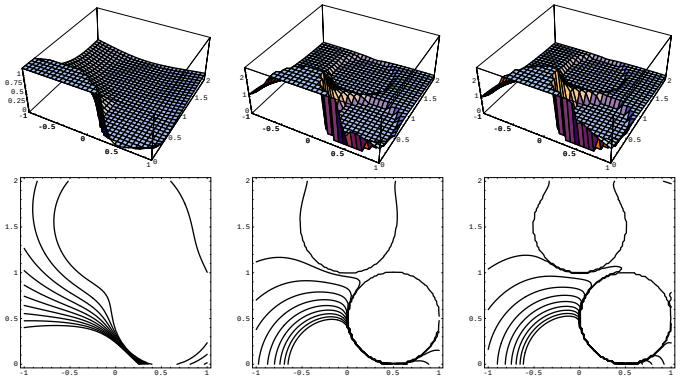

Fig. 21. Shape of an ILF for parameter k being $1, 5, 10$ (left to right).

Consider the case of a two dimensional workspace with two disk shaped obstacles of radius $r = 0.5[m]$ centered at $(x, y) = (0.5[m], 0.5[m])$ and $(x, y) = (0[m], 1.5[m])$ respectively. This configuration creates a narrow corridor between these two obstacles. Using the same representation of the obstacle functions, and the same parameter values for both cases the aim is to construct a navigation function that can steer a system within this corridor. Figure 20 depicts the shape and the equipotential curves of a typical navigation function with parameter k ranging from 1 to 10. Figure 21 shows the behavior of the inverse counterpart. The ILF responds faster to tuning and is capable of generating converging paths through the corridor for smaller values of the tuning parameter.

F. Proof of Lemma 2

For $k = 2$ we have lemma 1. Let $k = 3$. Then for $\boldsymbol{f}^1$, $\boldsymbol{f}^2$ with $\Gamma_0 \setminus \{\mathbf{0}\} = \mathcal{M}^1 \cap \mathcal{M}^2$ and

$$\boldsymbol{f}^{(1,2)} = \begin{cases} \boldsymbol{f}^1, & \boldsymbol{x} \in (\Gamma_0 \setminus \{\mathbf{0}\}) \cup \mathcal{C}^1 \\ \boldsymbol{f}^2, & \boldsymbol{x} \in \mathcal{C}^2, \\ \mathbf{0}, & \boldsymbol{x} = \mathbf{0}. \end{cases}$$

we have that $\boldsymbol{f}^{(1,2)}$ is asymptotically stable on $\mathcal{M}^1 \cup \mathcal{M}^2 \cup \{\mathbf{0}\}$. On Γ_0, $\boldsymbol{f}^1$ and $\boldsymbol{f}^2$ point towards $\mathcal{C}^1$ and $\mathcal{C}^2$ respectively. Therefore, $\mathbf{f}_0$ on Γ_0 is pointing towards $\mathcal{C}^1 \cup \mathcal{C}^2$. Applying lemma 1 for $\boldsymbol{f}^{(1,2)}$ and $\boldsymbol{f}^3$, it follows that the vector field $\boldsymbol{f}^{(1,2,3)}$:

$$\begin{cases} \boldsymbol{f}^1, & \boldsymbol{x} \in ((\mathcal{M}^1 \cap \mathcal{M}^3) \cup (\mathcal{M}^1 \cap \mathcal{M}^2) \setminus \{\mathbf{0}\}) \cup \mathcal{C}^1 \\ \boldsymbol{f}^2, & \boldsymbol{x} \in ((\mathcal{M}^2 \cap \mathcal{M}^3) \setminus \{\mathbf{0}\}) \cup \mathcal{C}^2 \\ \boldsymbol{f}^3, & \boldsymbol{x} \in \mathcal{C}^3, \\ \mathbf{0}, & \boldsymbol{x} = \mathbf{0}. \end{cases}$$

is globally asymptotically stable. Assume that lemma 2 holds for $k = n$. Then similarly the field $\boldsymbol{f}$:

$$\begin{cases} \boldsymbol{f}^1, & \boldsymbol{x} \in ((\mathcal{M}^1 \cap \mathcal{M}^3) \cup \cdots \cup (\mathcal{M}^1 \cap \mathcal{M}^n) \setminus \{\mathbf{0}\}) \cup \mathcal{C}^1 \\ \vdots & \\ \boldsymbol{f}^n, & \boldsymbol{x} \in ((\mathcal{M}^n \cap \mathcal{M}^{n+1}) \setminus \{\mathbf{0}\}) \cup \mathcal{C}^n \\ \boldsymbol{f}^n, & \boldsymbol{x} \in \mathcal{C}^n, \\ \mathbf{0}, & \boldsymbol{x} = \mathbf{0}. \end{cases}$$

is globally asymptotically stable. By induction follows that lemma 2 holds for every k.

G. Proof of Proposition 2

The functions $\mathrm{sign}(\cdot)$ and $\mathrm{atan2}(\cdot, \cdot)$ are defined as:

$$\mathrm{sign}(x) \triangleq \begin{cases} 1, & x \geq 0 \\ -1, & x < 0 \end{cases}, \quad \mathrm{atan2}(y, x) \triangleq \arg(x, y),$$

Consider the partition of the configuration space $\mathcal{Q} = \mathcal{C}^1 \oplus \cdots \oplus \mathcal{C}^{2k} \oplus \Gamma$ induced by the navigation function $V(\boldsymbol{q}) = V^j(\boldsymbol{q})$ for $\boldsymbol{q} \in \mathcal{C}^j, \quad j = 1, \ldots, 2k$. Then the time derivative $\dot{V}^j(\boldsymbol{q})$ of $V(\boldsymbol{q})$ in $\mathcal{C}^j$ is:

$$\sum_{r=1}^{k} \frac{k_v |f_{x_r} \cos\theta_r + f_{y_r} \sin\theta_r| \|\boldsymbol{f}\| + \omega_r f_{\theta_r} + \frac{\partial V^j}{\partial \boldsymbol{q}_{a_r}} \mathsf{K}_a \left(\frac{\partial V^j}{\partial \boldsymbol{q}_{a_r}}\right)^T}{\left(\sum_p \|\boldsymbol{h}_2^p\|^2\right)^2}$$

If $w_r \geq 0$, then $\omega_r = k_o(\theta_{d_r} - \theta_r)$ and

$$v_r\left(\frac{\partial V^j}{\partial x_r}\cos\theta_r + \frac{\partial V^j}{\partial y_r}\sin\theta_r\right) + \omega_r \frac{\partial V^j}{\partial \theta_r} = \frac{w_r(\boldsymbol{q})}{\left(\sum_p \|\boldsymbol{h}_2^p\|^2\right)^2} \geq 0$$

If $w_r < 0$, then $\omega_r = -v_r(f_{x_r}\cos\theta_r + f_{y_r}\sin\theta_r)(f_{\theta_r})^{-1}$ which gives $v_r(\frac{\partial V^j}{\partial x_r}\cos\theta_r + \frac{\partial V^j}{\partial y_r}\sin\theta_r) + \omega_r \frac{\partial V^j}{\partial \theta_r} = 0$ Given K_a is positive definite, $\sum_{r=1}^{k} \left(\frac{\partial V^j}{\partial \boldsymbol{q}_{a_r}}\right) \mathsf{K}_a \left(\frac{\partial V^j}{\partial \boldsymbol{q}_{a_r}}\right)^T \geq 0$, and $\dot{V}^j(\boldsymbol{q})$ is positive semidefinite. Now let $\mathcal{S} \triangleq \{\boldsymbol{q} \in \mathcal{C}^j \cup \Gamma \mid \dot{V}^j(\boldsymbol{q}) = 0\}$. If there exists an invariant set $\Omega \in \mathcal{S}$ then in Ω, $v_r = \omega_r = 0, \forall r$. From (18) it follows that v_r vanishes only at the origin. By LaSalle's principle for $\frac{1}{\dot{V}^j(\boldsymbol{q})}$ on $\mathcal{C}^j \cup \Gamma$, asymptotic stability for the system is established on $\mathcal{M}^j \triangleq \mathcal{C}^j \cup \Gamma \setminus \{\mathbf{0}\}$. By lemma 2, the system is globally asymptotically stable.